damage range indicated by PL. The lower intensity of some peaks compared to the as-grown sample indicates a certain degree of damage and can be used to obtain information about the damage profile. Only if the PL intensity of a QW equals that of the as-grown sample no damage due to implantation is observed. For all QWs the ratio I_1/I_0 was determined. We define that a value of 0.1 indicates the damage range. TRIM simulations [5] were made using the SRIM 2000 version, with full cascades as type of damage calculation. Fig. 2 shows the calculated vacancy profiles for implantation energies of 20 and 50keV. The maxima of the profiles correspond to some 10^{20} vacancies cm^{-3} at the dose 4×10^{13} He^+ ions cm^{-2}. The vacancy profile against the depth is shown, down to a vacancy concentration of $\sim 10^{16} cm^{-3}$ (limit of the TRIM calculation). Such a vacancy concentration can still initiate gradual degradation of GaAs-based laser diodes during ageing [6]. In the following, we take as penetration depth the depth where the vacancy concentration drops to $10^{16} cm^{-3}$. In Fig. 3, these penetration depths are depicted against the implantation energy. These values are contrasted with the damage range determined from the PL measurements. Appropriately we take the range corresponding to the lowest detectable PL intensity ratio I_1/I_0 of 0.1 (see inset to Fig. 3) and we find a good agreement with the TRIM results, e.g. at our maximum implantation energy of 50keV, the PL-relevant damage due to implantation reaches a depth of ~675nm, which compares well with the calculated depth of 700nm.

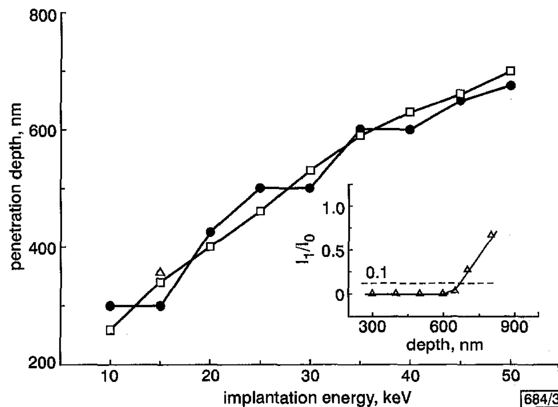

Fig. 3 *Damage penetration depth against He ion energy, determined from PL QW method and TRIM simulations*

$^4He^+$ implantation dose $4 \times 10^{13} cm^{-2}$
Lines are guides to the eyes
● PL QW
□ TRIM
Inset: PL intensity ratio I_1/I_0 against depth for E_{ion} = 50keV

Conclusion: Using the PL QW technique we were able to determine the damage depths of practically relevant He implantations at different energies in the GaAs/AlGaAs system. Contrasting the damage range corresponding to a reduction of PL QW intensity to 0.1 with the penetration depth of He atoms determined from TRIM simulations, we obtained a very good agreement between both values. It was demonstrated that TRIM is a suitable tool to predict the penetration depth of isolation implantations in laser diode structures and accordingly to determine the optimum technological parameters.

Acknowledgments: The authors thank A. Knauer for the growth, H. Kantwerk and G. Schöne for assistance, and H. Wenzel, U. Zeimer, M. Weyers and G.Tränkle for useful discussions.

© IEE 2001

5 February 2001
Electronics Letters Online No: 20010298
DOI: 10.1049/el:20010298

S. Gramlich, E. Nebauer, J. Sebastian and G. Beister (*Ferdinand-Braun-Institut für Höchstfrequenztechnik, Albert-Einstein-Straße 11, D-12489 Berlin, Germany*)

References

1 ZEIMER, U., and NEBAUER, E.: 'High resolution X-ray diffraction investigation of He-implanted GaAs', *Semicond. Sci. Technol.*, 2000, **15**, pp. 965–970

2 BERTOLET, D., HSU, J., and LAU, K.: 'AlGaAs/GaAs quantum wells with high carrier confinement and luminescence efficiencies by organometallic chemical vapor deposition', *J. Appl. Phys.*, 1987, **62**, pp. 120–125

3 DENBAARS, S., DAPKUS, C., BEYLER, A., HARIZ, A., and DZUCKO, M.: 'Atomic layer epitaxy for the growth of heterostructure devices', *J. Cryst. Growth*, 1988, **91**, pp. 195–200

4 RESSEL, P., STRUSNY, H., GRAMLICH, S., ZEIMER, U., SEBASTIAN, J., and VOGEL, K.: 'Optimised proton implantation step for vertical-cavity surface-emitting lasers', *Electron. Lett.*, 1993, **29**, pp. 918–919

5 ZIEGLER, J.F., BIERSACK, J.P., LITTMARK, U.: 'The stopping and range of ions in solids' (Pergamon Press, New York, 1985)

6 HAYASHI, J.: 'Degradation in III-V-opto-electronic devices', *J. Phys. Soc. Japan, Suppl. A*, 1980, **49**, pp. 57–65

Electron *g* factor engineering in III-V semiconductors for quantum communications

H. Kosaka, A.A. Kiselev, F.A. Baron, Ki Wook Kim and E. Yablonovitch

An entanglement-preserving photodetector converts photon polarisation to electron spin. Up and down spin must respond equally to oppositely polarised photons, creating a requirement for degenerate spin energies, $g_e \simeq 0$, for electrons. The authors present a plot of g_e factor against lattice constant, analogous to bandgap against lattice constant, that can be used for g factor engineering of III-V alloys and quantum wells.

The major reason for researching III-V semiconductors has been the development of opto-electronic devices for optical communications. One of the key inventions for improved semiconductor lasers was electronic band structure engineering based on strained heterostructures [1]. Practical realisation of quantum communications [2, 3] is expected to require entanglement-preserving photodetectors in which quantum information is transmitted by photon polarisation through an optical fibre, and then transferred to electron spin in a semiconductor [4, 5]. To maintain the entanglement, the photodetector should absorb equally into up and down electron spin states, and thus the electron g factor should be engineered for $g_e \simeq 0$. Fortunately, the familiar band structure engineering of effective mass can equally well control the g factor as well. There are additional requirements in [5] for moderately long spin coherence times, and for a hole g factor $|g_h| \gg 0$, large enough to lift the Kramers' degeneracy of the valence band. Various III-V alloys and quantum wells can be engineered to produce the right g factor combinations.

To commence the task of g factor engineering, we have graphed the experimental electron g_e factors in III-V semiconductors as a function of the lattice constant Fig. 1. This is analogous to the famous graph of bandgaps against lattice constant plotted in Fig. 2. In these Figures, the vertical and horizontal dash-dotted lines illustrate the design preferences. The horizontal axis in Fig. 1 shows the requirement for the zero electron g_e factor $g_e \simeq 0$. The horizontal dash-dotted line in Fig. 2 shows a preference for a bandgap of 0.8eV, or λ = 1.55μm, corresponding to the optimum wavelength for fibre optic communications, but shorter wavelengths λ = 1.3μm are also acceptable for quantum communication. To lattice match the entanglement-preserving photodetector to a conventional InP substrate, a vertical dash-dotted line is shown at lattice constant a = 5.86Å.

To fill in the gaps between the experimental g_e factor points in Fig. 1, some theoretical curves are included. The following simple formula derived from the k·p perturbation theory [6] was used for the theoretical curves:

$$g_e = 2 - \frac{2}{3}\frac{E_p \Delta}{E_g(E_g + \Delta)} \quad (1)$$

where E_g is the energy bandgap, Δ is the spin-orbit splitting energy, and E_p is the energy equivalent of the principal interband momentum matrix element. We used experimentally determined E_g, and linearly interpolated Δ and E_p for alloys, utilising known

values for pure compounds. No fitting parameters were used. Although the formula includes only the lowest conduction band, the highest valence band, and a spin split-off valence band, it agrees reasonably well with the experimental data. The dotted lines in the Figure show the range of indirect material, where eqn. 1 is not applicable, and $g_{e,indirect} \simeq 2$.

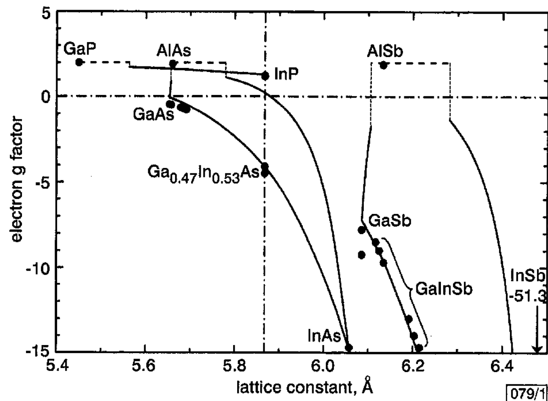

Fig. 1 *g_e factors for conduction electrons in III-V semiconductors against lattice constant*

● experimental g_e factors
——— direct bandgap (theory)
- - - - indirect bandgap (theory)
— · — lattice constant of bulk InP (normally used for optical communication devices)
Bulk g_e factors are plotted for direct bandgap materials (InP [7, 8], GaAs [9], GaInAs [10 – 12], InAs [13], GaSb [14, 15], GaInSb [16] and InSb [17]), and defect or impurity related g factors are plotted for indirect bandgap materials (GaP [18], AlAs [19], and AlSb [20])
T = 1.4–4.2K, ([13] is taken at 30K)

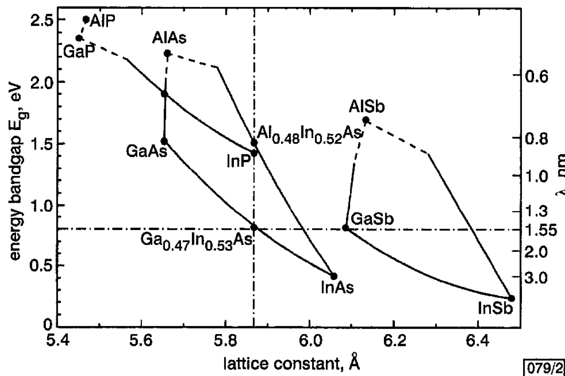

Fig. 2 *Energy bandgaps for materials shown in Fig. 1 at temperatures between 1.4 and 4.2K*

The trend in both Figs. 1 and 2 is for the g_e factor to be more negative as the bandgap drops. The main exception is InP. InP is the only III-V to show a positive g_e factor at moderate bandgaps. This is because of the remarkably small spin-orbit splitting Δ = 0.108eV in InP. Considering only bulk III-V semiconductors, it is preferable to reduce E_g down to 0.8eV (1.55μm), while keeping Δ no larger than 0.11eV, in order to achieve a near-zero g_e factor (E_p is always around 22eV). No bulk material is readily available with these characteristics. Much more design freedom can be achieved in multilayer heterostructures. For a reliable quantitative analysis to establish a proper design, it is necessary to take into account the effects of quantum confinement as well as the strain-induced valence band splitting to fulfill the electron and hole g factor requirements of an entanglement-preserving photodetector.

Acknowledgment: This project is sponsored by the Defense Advanced Research Projects Agency & Army Research Office projects MDA972-99-1-0017, DAAD19-00-1-0172, and MDA972-00-1-0035.

© IEE 2001
2 November 2000
Electronics Letters Online No: 20010314
DOI: 10.1049/el:20010314

H. Kosaka, E. Yablonovitch and F.A. Baron (*University of California, Los Angeles, Electrical Engineering Department, Los Angeles, California 90024, USA*)

E-mail: hideok@ee.ucla.edu

A.A. Kiselev and Ki Wook Kim (*Department of Electrical and Computer Engineering, North Carolina State University, Raleigh, North Carolina 27695, USA*)

H. Kosaka: On leave from NEC

References

1 YABLONOVITCH, B., and KANE, E.O.: 'Band structure engineering of semiconductor lasers for optical communications', *J. Lightwave Technol.*, 1988, **6**, (8), pp. 1292-1299

2 BENNETT, C.H., and BRASSARD, G.: 'The dawn of a new era for quantum cryptography; The experimental prototype is working!', *SIGACT News*, 1989, **20**, pp. 78–82

3 BENNETT, C.H., and WIESNER, S.J.: 'Communication via one- and two-particle operators on Einstein-Podolsky-Rosen states', *Phys. Rev. Lett.*, 1992, **69**, pp. 2881–2884

4 VRIJEN, R. *et al.*: 'Electron spin resonance transistors for quantum computing in Silicon-Germanium hetero-structures', *Phys. Rev. A*, 2000, **62**, (1), pp. 012306-1–10

5 VRIJEN, R., and YABLONOVITCH, B.: 'A solid-state spin coherent photo-detector for quantum communication', to be published in *Physica E*

6 ROTH, L.M., LAX, B., and ZWERDLING, S.: 'Theory of optical magneto-absorption effects in semiconductors', *Phys. Rev.*, 1959, **114**, (1), pp. 90–100

7 WEISBUCH, C., and HERRMANN, C.: 'Optical detection of conduction electron spin resonance in InP', *Solid State Commun.*, 1975, **16**, (5), pp. 659–661

8 OESTREICH, M., HALLSTEIN, S., HEBERLE, A.P., EBERL, L., BAUSER, B., and RUHLE, W.W.: 'Temperature and density dependence of the electron Lande g factor in semiconductors', *Phys. Rev. B*, 1996, **53**, (12), pp. 7911–7916

9 WHITE, A.A., HINCHLIFEE, J., and DEAN, P.J.: 'Zeeman spectra of the principal bound exciton in Sn-doped gallium arsenide', *Solid State Commun.*, 1972, **10**, (6), pp. 497–500

10 WEISBUCH, C., and HERRAUN, C.: 'Optical detection of conduction-electron spin resonance in GaAs, $Ga_{1-x}In_xAs$, and $Ga_{1-x}Al_xAs$', *Phys. Rev. B*, 1977, **15**, (2), pp. 816–822

11 KOWALSKI, B., OMLING, P., MEYER, B.K., HOFMANN, D.M., HÄRLE, V., SCHOLZ, F., and SOBKOWICZ, P.: 'Optically detected spin resonance of conduction band electrons in InGaAs/InP quantum wells', *Semicond. Sci. Technol.*, 1996, **11**, pp. 1416–1423

12 DOBERS, M., VIEREN, J.P., and GULDNER, Y.: 'Electron-spin resonance of the two-dimensional electron gas in $Ga_{0.47}In_{0.53}As$-InP heterostructures', *Phys. Rev. B*, 1989, **40**, (11), pp. 8075–8078

13 KONOPKA, J.: 'Conduction electron spin resonance in InAs', *Phys. Lett.*, 1967, **26A**, p. 29

14 HERMANN, C., and WEISBUCH, C.: 'k·p perturbation theory in III-V compounds and alloys: a reexamination', *Phys. Rev. B*, 1977, **15**, (2), pp. 823–833

15 REINE, M., AGGARWAL, R.L., and LAX, B.: 'Stress-modulated magnetoreflectivity of gallium antimonide and gallium arsenide', *Phys. Rev. B*, 1972, **5**, (8), pp. 3033–3049

16 ROTH, A.P., and FORTIN, E.: 'Interband magneto-optical study of the $In_{1-x}Ga_xSb$ alloy system', *Can. J. Phys.*, 1978, **56**, (11), pp. 1468–1475

17 ISAACSON, R.A.: 'Electron spin resonance in n-type InSb', *Phys. Rev.*, 1968, **169**, pp. 312

18 KAUFMANN, U., SCHNEIDER, J., and RAUBER, A.: 'ESR detection of antisite lattice defects in GaP, $CdSiP_2$ and $ZnGeP_2$ ', *Appl. Phys. Lett.*, 1976, **29**, (5), pp. 312–313

19 GLASER, E.R., KENNEDY, T.A., MOLNAR, B., and SILLMON, R.S.: 'Optically detected magnetic resonance of group-IV and group-VI impurities in AlAs and $Al_xGa_{1-x}As$ with x > 0.35', *Phys. Rev. B*, 1991, **43**, (18), pp. 14540–14556

20 GLASER, E.R., KENNEDY, T.A., BENNETT, B.R., and SHANABROOK, B.V.: 'Strong emission from As monolayers in AlSb', *Phys. Rev. B*, 1999, **59**, (3), pp. 2240–2244